In situ XAS study of $Li_xNi_{0.7}Fe_{0.15}Co_{0.15}O_2$ cathode material

Azzam N. Mansour,[a*] Laurence Croguennec,[b] G. Prado[b] and Claude Delmas[b]

[a]*Naval Surface Warfare Center, Carderock Division, 9500 MacArthur Boulevard, West Bethesda, MD 20817-5700, USA,* [b]*Institut de Chimie de la Matière Condensée de Bordeaux-CNRS and Ecole Nationale Supérieure de Chimie et Physique de Bordeaux, Château de Brivazac, Av. Dr A. Schweitzer, 33608 Pessac Cedex, France.*
[*]*Email: MansourAN@nswccd.navy.mil*

We have examined the oxidation states and local atomic structures of Ni, Fe, and Co in $Li_xNi_{0.7}Fe_{0.15}Co_{0.15}O_2$ as a function of Li content during the first charge in a $Li//Li_xNi_{0.7}Fe_{0.15}Co_{0.15}O_2$ nonaqueous cell. We show that the composition of the material in the pristine state is more accurately described by $Li_{0.95}Ni(II)_{0.09}Ni(III)_{0.66}Fe(III)_{0.15}Co(III)_{0.15}O_2$. Half of the Ni(II) resides in Li-vacant sites. Both Fe and Co substitute for Ni within the NiO_2 slabs with no significant amounts of Fe or Co that can be attributed to Li-vacant sites. The local structure parameters are consistent with oxidation states observed on the basis of the XANES data. The Ni K-edge energy continuously shifts to a higher energy with decrease in Li content due to oxidation of Ni(II) to Ni(III) and Ni(III) to Ni(IV). After the complete oxidation of Ni(III) to Ni(IV), the Fe K-edge energy begins to increase with further decrease in Li content indicating the oxidation of Fe(III) to Fe(IV). The Co K-edge energy at half-height, on the other hand, is unchanged during the whole range of Li deintercalation indicating that no significant change in the oxidation state of Co occurs upon the complete removal of Li.

Keywords: lithium nickel oxide, in situ, x-ray absorption spectroscopy, structure, oxidation state, intercalation materials, metal substitution, lithium batteries.

1. Introduction

$LiNiO_2$ is a promising cathode material for Li batteries due to its lower cost and toxicity relative to the currently used $LiCoO_2$. However, it is well known that the electrochemical performance of $LiNiO_2$ strongly depends on preparation procedures such as precursors and heat treatment conditions (Ohzuku et al., 1993; Rougier et al., 1996). Various preparation procedures commonly produce non-stoichiometric phases better described by the formula $Li_{1-z}Ni_{1+z}O_2$ where z represents the fraction of Li sites occupied by Ni(II) (Rougier et al., 1996). The formation of non-stoichiometric phases leads to poor capacity retention. In order to improve electrochemical performance, the effect of partial transition metal substitution on cation distribution has been examined (Delmas & Saddoune, 1992; Rougier et al., 1996b).

Recently (Mansour et al., 1999a; 1999b; 2000), the evolution of the oxidation state and local structure of Ni in $Li_{1-z}Ni_{1+z}O_2$ during redox reactions was explored by *in situ* x-ray absorption spectroscopy (XAS). The objective of this paper is to examine the evolution of the oxidation states and local structures of Ni, Fe, and Co during the first charge of a $Li//Li_xNi_{0.7}Fe_{0.15}Co_{0.15}O_2$ nonaqueous cell by in situ XAS.

2. Experiment

Methodology for preparation of the cathode was described elsewhere (Mansour et al., 2000). The XAS experiment was performed on beamline X-11A at NSLS with the electron storage ring operating at energy of 2.58 GeV and a current in the range 110-350 mA. The XAS data were collected continuously during the first charge of the $Li//Li_xNi_{0.7}Fe_{0.15}Co_{0.15}O_2$ cell in transmission mode using Si(111) double-crystal monochromator (35% detuned) with energy resolution of 1.9 eV at the Ni K-edge energy. The change in Li-content per scan was kept near 0.02 during the collection of the combined Fe, Co, and Ni K-edge spectra. A 4 μm thick Ni foil was used as an internal reference for energy calibration. The K-edge absorption jumps for the cathode are 0.33, 0.30, and 1.17 for Fe, Co, and Ni, respectively.

The EXAFS spectrum, $\chi(k)$, was extracted using a cubic spline procedure, which minimized the amplitude of non-physical peaks in the 0-1 Å region of the Fourier transform. The spectra were normalized to a per atom basis using the absorption step at 100 eV above the edge energy. Energy dependent normalization was also applied to the $\chi(k)$ data using the atomic absorption calculated with McMaster coefficients. Theoretical standards based on the curved-wave scattering formalism of the FEFF Code (Zabinsky et al. 1995) were used in fitting the EXAFS data. All fits were performed in real space (ΔR: 0.8-3.1 Å) using the curve fitting code FEFFIT of the UWXAFS package (Stern et al., 1995). Fourier transforms were generated using the k-ranges 4-13, 4-12, 4-11 $Å^{-1}$ for Ni, Co, and Fe, respectively. A three-shell fit was required to analyze the Ni K-edge data for $x > 0.47$. The first two shells accounted for the distorted octahedral-coordination of the Ni-O sphere and the third shell accounted for the Ni-Ni/Co/Fe sphere. In this fit, the total number of Ni-O bonds was constrained to be equal to 6 and all were assumed to have the same disorder. For $x < 0.47$, a two shell-fit was sufficient to analyze the Ni-K-edge data. One shell accounted for the Ni-O sphere and the other one accounted for the Ni-Ni/Co/Fe sphere. A two-shell fit was sufficient to analyze both the Co and the Fe K-edge data over the full range of compositions, in order to account for the first and second coordination spheres. In the case of Co, the coordination numbers, distances, and disorders were used as floating parameters. In the case of Fe, a high degree of structural disorder was realized and the data were fitted by constraining the coordination numbers for both shells to 6 and using the third and fourth terms of the cumulant expansion for each shell as additional floating parameters. One inner potential (E_0) was used as a floating parameter in all fits. The amplitude of the many body reduction factor (S_o^2) was determined to be 0.84 for Ni and Fe and 0.83 for Co from XAFS spectra of their respective foils.

3. Results and Discussion

The phase uncorrected Fourier transforms of the k^3-weighted EXAFS spectra for the Ni, Fe, and Co K edges are shown in Figures 1, 2, and 3, respectively. The Fourier transforms for Ni, Fe, and Co are similar in nature and are consistent with the layered structure of the material. The amplitudes of various peaks are due to scattering contributions mainly within the Ni/Fe/Co-O_2 slabs with no significant contribution from the interslabs. Clearly, the local structures of Ni and Fe are significantly perturbed while that of Co is not notably perturbed during the Li deintercalation.

A summary of local structure parameters only for the fully discharged and charged states due to space limitations is shown in Table I. Variations in the Ni local structure parameters with composition for this sample are similar to those observed for nearly stoichiometric $Li_{1-z}Ni_{1+z}O_2$ (Mansour et al., 2000). On the basis of the Ni-O coordination, we conclude that in the fully discharged state Ni is present mainly as Ni(III) in the NiO_2 slabs with a small fraction as Ni(II) distributed equally between the NiO_2 slabs and Li-vacant sites. The presence of Ni(II) in Li-vacant sites is also supported by the Ni-Ni coordination, which is higher than 6 as a result. A value of 6 is indicative of stoichiometric phases. The fraction of Ni(II) residing in Li-vacant sites is estimated to be 0.067 ± 0.026. Hence,

the composition in the pristine state is more accurately represented by $Li_{0.95}Ni(II)_{0.09}Ni(III)_{0.66}Fe(III)_{0.15}Co(III)_{0.15}O_2$. Variations in the amplitude and position of the Ni-O contribution vs. Li content are consistent with oxidation of Ni(II) to Ni(III) and Ni(III) to Ni(IV). As has been shown earlier (Rougier et al., 1995), Ni(III) has a distorted octahedral coordination with 4 and 2 oxygen atoms at 1.92 and 2.06 Å, respectively. Ni(IV), on the other hand, has a regular octahedral coordination with 6 oxygen atoms at 1.88 Å. Hence, the amplitude of the Ni(III)-O contribution is significantly reduced relative to that of the Ni(IV) contribution due to a destructive interference between the short and long distance contributions for Ni(III). After the complete removal of Li, the Ni-O and Ni-Ni distances decreased to 1.88 and 2.82 Å, respectively, which are characteristic of Ni(IV). Assuming the absence of cation mixing, no significant amounts of Fe or Co can be attributed to Li-vacant sites. The observed Fe-O distance in the discharged state is consistent with the sum of the ionic radii for Fe(III) and O^{2-} (Shannon, 1976). The observed Fe-O distance in the charged state is somewhat smaller than the sum of the ionic radii for Fe(IV) and O^{2-} (Shannon, 1976) but is similar to the Ni(IV)-O distance. Thus, Fe is present as Fe(III) in the discharged state and as Fe(IV) in the charged state. The Co-O distance in the discharged state is consistent with that in $LiCoO_2$ and that in the charged state is slightly smaller than the Co(IV)-O distance in CoO_2. However, the Co(III)-O distance in $LiCoO_2$ (Reimers & Dahn, 1992) is similar to the Co(IV)-O distance in CoO_2 (Amatucci et al., 1996) and hence, oxidation state determination for Co can not be made on the basis of the Co-O distance. We believe that the observed contraction in the Co-O distance in the charged state is dictated by the host lattice rather than oxidation of Co(III) to Co(IV).

The Ni, Fe, and Co K-edge XANES as a function of Li content are shown in Figures 4, 5, and 6, respectively. The XANES for $KNiIO_6$ is also included in Figure 4 as a reference for tetravalent Ni. The Ni K-edge energy continuously shifts to higher energy upon removal of Li. The largest energy shift is observed for x = 0.27. No additional increase in the Ni K-edge energy is observed upon further removal of Li. The energy shift in going from x =1 to x = 0.27 or x = 0.0 (x in $Li_xNi_{0.7}Fe_{0.15}Co_{0.15}$) is 1.67 ± 0.14 eV. The increase in the Ni K-edge energy is consistent with oxidation of Ni(III) to Ni(IV) as evidenced by comparison with the XANES for tetravalent Ni in $KNiIO_6$.

Table 1
Summary of local atomic structure parameters for $Li_xNi_{0.7}Fe_{0.15}Co_{0.15}O_2$.

x	X-Y Pair	N	R (Å)	$\sigma^2(10^{-3}$ Å$^2)$
0.95	Ni-O	3.5±0.3	1.91±0.01	4.2±0.8
		2.5±0.3	2.05±0.01	4.2±0.8
	Ni-Ni	6.6±0.3	2.880±0.003	4.9±0.3
	Fe-O†	6.0	2.03±0.02	5.5±1.7
	Fe-Fe†	6.0	2.94±0.03	5.7±1.4
	Co-O	5.8±0.6	1.924±0.004	2.3±0.8
	Co-Co	6.0±0.6	2.870±0.004	3.4±0.7
0.0	Ni-O	5.4±0.4	1.88±0.01	2.6±0.6
	Ni-Ni	5.3±0.3	2.817±0.003	2.9±0.4
	Fe-O†	6.0	1.88±0.04	11.6±2.9
	Fe-Fe†	6.0	2.85±0.05	12.5±2.8
	Co-O	6.3±0.7	1.881±0.005	3.6±0.9
	Co-Co	5.0±0.5	2.819±0.005	1.8±0.6

† Coordination number was constrained to 6.0 while the 3rd and 4th terms of the cumulant expansion used as variables in the fit. For x = 0.95: $C^3_{Fe\text{-}O}$ = 0.00029 ± 0.00032 Å^3, $C^3_{Fe\text{-}Fe}$ = 0.00049 ± 0.00033 Å^3, $C^4_{Fe\text{-}O}$ = 0.000023 ± 0.000072 Å^4, and $C^4_{Fe\text{-}Fe}$ = 0.000018 ± 0.000050 Å^4. For x = 0.0: $C^3_{Fe\text{-}O}$ = – 0.00032 ± 0.00053 Å^3, $C^3_{Fe\text{-}Fe}$ = 0.00022 ± 0.00062 Å^3, $C^4_{Fe\text{-}O}$ = 0.00019 ± 0.00011 Å^4, and $C^4_{Fe\text{-}Fe}$ = 0.00017 ± 0.00010 Å^4.

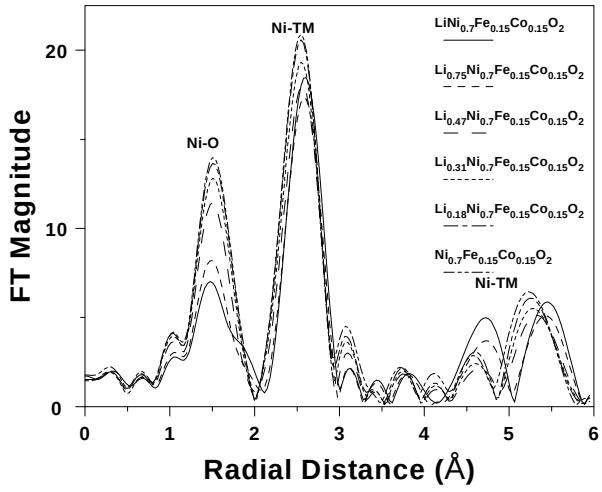

Figure 1
Fourier transforms of Ni K-edge EXAFS for $Li_xNi_{0.7}Fe_{0.15}Co_{0.15}O_2$.

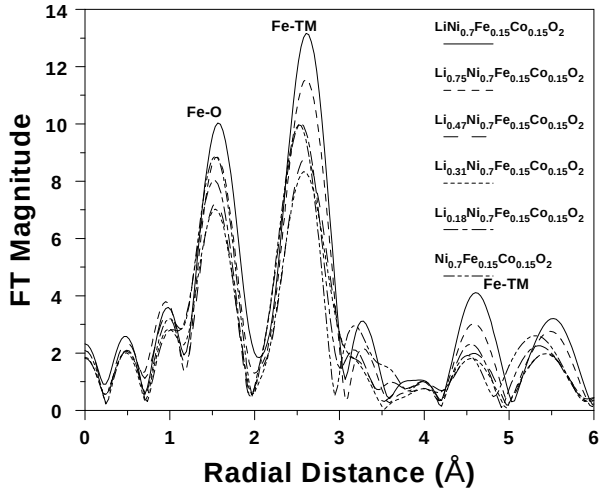

Figure 2
Fourier transforms of Fe K-edge EXAFS for $Li_xNi_{0.7}Fe_{0.15}Co_{0.15}O_2$.

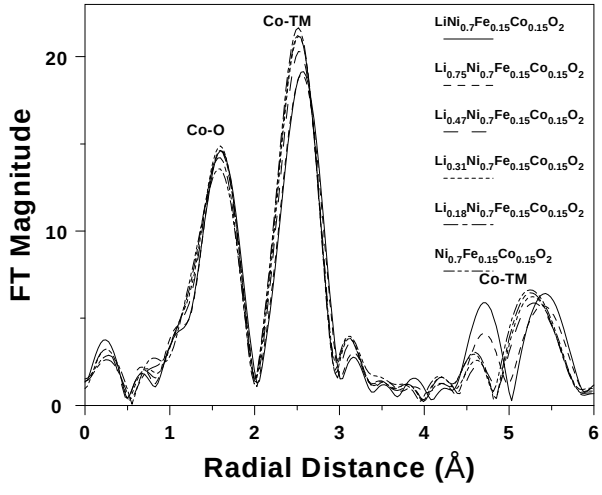

Figure 3
Fourier transforms of Co K-edge EXAFS for $Li_xNi_{0.7}Fe_{0.15}Co_{0.15}O_2$.

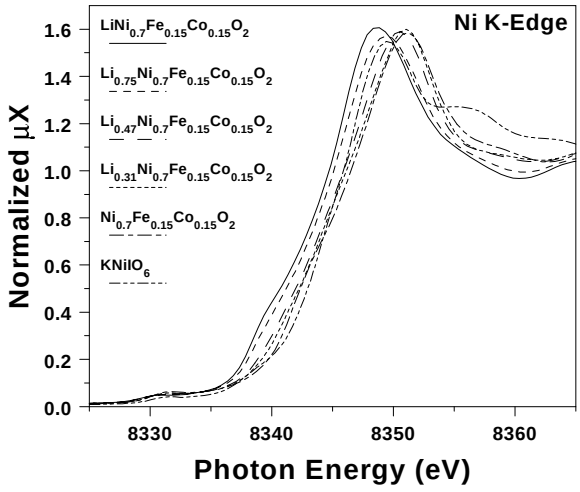

Figure 4
Ni K-edge XANES for $Li_xNi_{0.7}Fe_{0.15}Co_{0.15}O_2$ as a function of Li content along with that for $KNiIO_6$ as reference for tetravalent Ni.

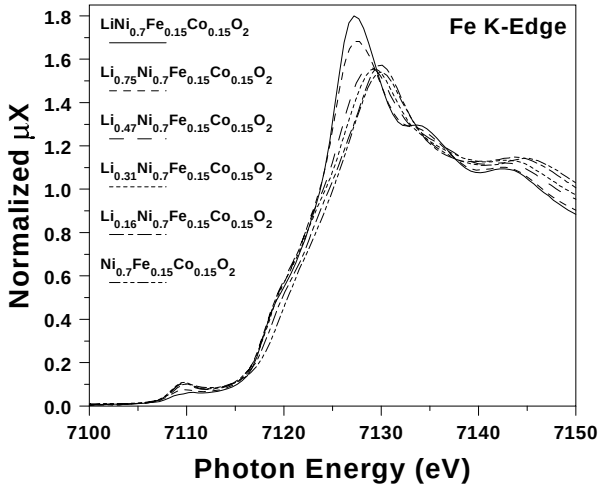

Figure 5
Fe K-edge XANES for $Li_xNi_{0.7}Fe_{0.15}Co_{0.15}O_2$ as a function of Li content.

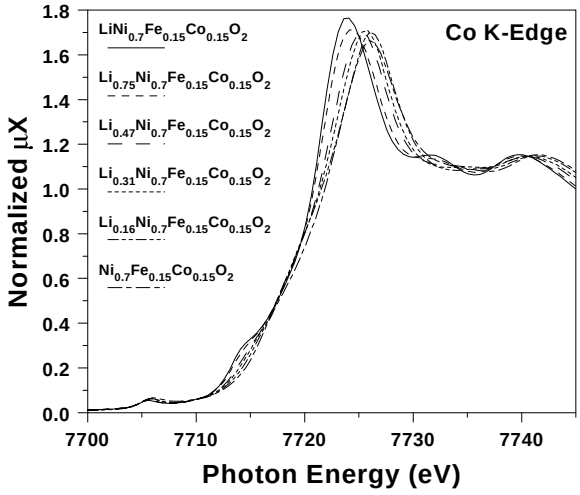

Figure 6
Co K-edge XANES for $Li_xNi_{0.7}Fe_{0.15}Co_{0.15}O_2$ as a function of Li content.

The Fe K-edge energy is unchanged with decreases in Li content down to x = 0.27 if one examines the region at the onset of the edge where the absorption intensity is less than 1. The Fe K-edge energy, however, increases with further decreases in lithium content down to x = 0.0. The observed Fe shift in going from $LiNi_{0.7}Fe_{0.15}Co_{0.15}O_2$ to $Ni_{0.7}Fe_{0.15}Co_{0.15}O_2$ is 1.00 ± 0.14 eV, which presumably due to oxidation of Fe(III) to Fe(IV). This shift is much smaller than the observed energy shifts in going from Mn(III) to Mn(IV) or Ni(III) to Ni(IV) (Mansour, 1999a). However, a similar shift in going from Fe(III) to Fe(IV) was observed upon oxidation of Fe-containing nickel hydroxides (Balasubramanian et al., 2000). Thus, the oxidation of Fe (III) to Fe(IV) occurs after the complete oxidation of Ni(III) to Ni(IV).

The trends we observe in the Co K-edge XANES are similar to those reported for $Li_xNi_{0.5}Co_{0.5}O_2$ in an earlier study (Nakai & Nakagome, 1998). The Co K-edge energy (at half-height) is unchanged upon removal of all of the Li indicating that the oxidation state of Co remained at +3 independent of composition. The pre-edge peak energy vs. x also supports this conclusion. The intensity of the pre-edge peak, however, increases with decreases in Li content. This is consistent with an increase in the degree of hybridization between the Co 3*d*, Co 4*p*, and O 2*p* states with decreases in Li content.

Based on the composition deduced from the EXAFS results $Li_{0.95}Ni(II)_{0.09}Ni(III)_{0.66}Fe(III)_{0.15}Co(III)_{0.15}O_2$, it is impossible to oxidize all of the Ni, Fe, and Co. Removal of Li to x = 0.16 should in principle oxidize all of the Ni. Further removal of Li to x = 0 should oxidize either (i) all of the Fe, (ii) all of the Co, or (iii) half of the Fe and half of the Co. On the basis of the XANES data, we believe that only Fe is oxidized after the complete oxidation of Ni(III) to Ni(IV).

The authors acknowledges financial support by ONR, ILIR Program of NSWCCD, CNES, SAFT, Région Aquitaine, and the US DOE under Contract # DE-AS05-80-ER-10742 for its role in the development and operation of beam line X-11A at NSLS. NSLS is supported by the US DOE under Contract # DE-AC02-76CH00016.

References

Amatucci, G. G., Tarascon, J. M. & Klein, L. C. (1996). J. Electrochem. Soc. 143(3), 1114-1123.
Balasubramanian, M., Melendres, C. A. & Mini S. (2000). J. Phys. Chem. B, 104(18), 4300-4306.
Delmas, C. & Saadoune I. (1992). Solid State Ionics, 53-56, 370-375.
Mansour, A. N., McBreen, J. & Melendres, C. A. (1999a). J. Electrochem. Soc. 146(8), 2799-2809.
Mansour, A. N., McBreen, J. & Melendres, C. A. (1999b). The Electrochem. Soc. Proc. Ser., PV99-16, 217-228.
Mansour, A. N., Yang, X. Q., Sun, X., McBreen, J., Croguennec, L. & Delmas, C. (2000). J. Electrochem. Soc. 147, 2104-2109.
Nakai, I. & Nakagome, T. (1998). Electrochem. Solid-State Lett. 1(6), 259-261.
Ohzuko, T., Ueda, A. & Nagayama, M. (1993). J. Electrochem. Soc. 140(7), 1862-1870.
Reimers, J. N. & Dahn, J. R. (1992). J. Electrochem. Soc. 139(8), 2091-2097.
Rougier, A., Gravereau, P. & Delmas, C. (1996a). J. Electrochem. Soc. 143(4), 1168-1175.
Rougier, A., Saadoune, I., Gravereau, P., Willmann P. & Delmas, C. (1996b). Solid State Ionics, 90, 83-90.
Rougier, A., Delmas, C. & Chadwick, A. V. (1995). Solid State Commun. 94(2), 123-127.
Shannon, R. D. (1976). Acta Cryst. A32, 751-767.
Stern, E. A., Newville, M., Ravel, B., Yacoby, Y. & Haskel, D. (1995). Physica B, 208&209, 117-120.
Zabinsky, S. I., Rehr, J. J., Ankudinov, A., Albers, R. C. & Eller, M. J. (1995). Phys. Rev. B,. 52, 2995-3009.